



CHALMERS
UNIVERSITY OF TECHNOLOGY

A synergistic two-stage process for rare earth element extraction from bastnasite leachates in ethylene glycol: The dual role of Cyanex 923 as a

Downloaded from: <https://research.chalmers.se>, 2026-06-06 13:13 UTC

Citation for the original published paper (version of record):

Kaplan, S., Sonmez, M., Petranikova, M. (2026). A synergistic two-stage process for rare earth element extraction from bastnasite leachates in ethylene glycol: The dual role of Cyanex 923 as a purification and process conditioning agent. *Chemical Engineering Journal Advances*, 26. <http://dx.doi.org/10.1016/j.ceja.2026.101183>

N.B. When citing this work, cite the original published paper.



A synergistic two-stage process for rare earth element extraction from bastnasite leachates in ethylene glycol: The dual role of Cyanex 923 as a purification and process conditioning agent

S.Samet Kaplan^{a,b}, M.Seref Sonmez^a, Martina Petranikova^{c,*}

^a Metallurgical and Materials Engineering Department, Faculty of Chemical and Metallurgical Engineering, Istanbul Technical University, 34469, Maslak, Istanbul, Turkey

^b Metallurgical and Materials Engineering Department, Faculty of Engineering and Natural Sciences, Hitit University, Corum, Turkey

^c Department of Chemistry and Chemical Engineering, Industrial Materials Recycling and Nuclear Chemistry, Chalmers University of Technology, Gothenburg, Sweden

ARTICLE INFO

Keywords:

Deep eutectic solvents (DES)
Green solvents
Rare Earth Elements
Extractive metallurgy

ABSTRACT

The recovery of rare earth elements (REE) using non-aqueous solvents provides a sustainable alternative to conventional hydrometallurgy, while enabling unique extraction mechanisms inherent to organic media. This study examines REE extraction from bastnasite ore leached in an ethylene glycol–FeCl₃ system. Among four different extractants evaluated, D2EHPA demonstrated exceptional selectivity for heavy REE, achieving a Y/Ce separation factor of 270.4. Following the extractant screening step, the loading and stripping conditions for D2EHPA were systematically optimized to maximize Y extraction efficiency. Optimized loading conditions enabled Y extraction to reach 97 % under 30 min. shaking time, 2000 rpm, and 2:1 E/L ratio. Y was stripped back with 3 M HNO₃ at a high recovery rate (87.4 %), but substantial iron co-extraction necessitated an additional purification step. Therefore, a pre-treatment stage using C923 was implemented, achieving an iron scavenging efficiency of over 95 %. Beyond simple purification, this step revealed a novel in-situ chemical conditioning mechanism. As confirmed by FTIR spectroscopy—which showed an intensified free-water band (~1650 cm⁻¹) resulting from HFeCl₄ solvation and subsequent proton consumption—C923 inherently reduced the extreme acidity of the non-aqueous matrix. This base-free pH modification eliminated the precipitation challenges common in aqueous systems and successfully "unlocked" D2EHPA to co-extract light REE alongside heavy REE. Such an outcome was previously impossible in the raw acidic leachate. Overall, the study establishes two operational pathways: a highly selective Y extraction route using D2EHPA alone, and a synergistic bulk REE recovery route enabled by the dual purification and acidity-conditioning functions of C923.

1. Introduction

The extraction of REE from primary ores has gained significant momentum in recent years due to the increasing demand for these critical materials in high-technology applications. Comprehensive review articles have highlighted the shift towards optimizing extraction processes from primary sources to ensure a sustainable supply chain [1–3]. Among these sources, bastnasite remains the most commercially significant REE mineral, necessitating the development of efficient and environmentally friendly hydrometallurgical routes. Unlike traditional aqueous methods, non-aqueous based-leaching system promotes sustainability by minimizing water consumption, along with other advantages described in the literature [4,5]. Among various green solvents,

particularly deep eutectic solvents (DES) used in metal extraction [6,7], ethylene glycol (EG) combined with metal chlorides (e.g. FeCl₃, CuCl₂, ZnCl₂) has gained considerable attention [8,9] due to its high extraction efficiency and ease of preparation. However, this EG + MCl leaching mechanism inherently yields a pregnant leach solution (PLS) saturated with the leaching metal ion, creating a complex matrix that requires a tailored separation strategy. To address this issue and clear the PLS of metal ions, C923 which is a neutral extractant composed of four different trialkylphosphine oxides is a potential extractant [10,11].

REE extraction from ore leachates generally starts with separating heavy REE (HREE) and light REE (LREE). Although C923 is capable of extracting yttrium (one of HREE) from neutral nitrate media [12], its affinity for trivalent REE in acidic chloride media is significantly lower

* Corresponding author.

E-mail addresses: ssametkaplan@hitit.edu.tr (S.Samet Kaplan), ssonmez@itu.edu.tr (M.Seref Sonmez), martina.petranikova@chalmers.se (M. Petranikova).

<https://doi.org/10.1016/j.cej.2026.101183>

Available online 7 April 2026

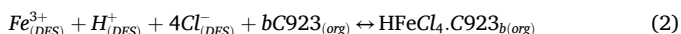
2666-8211/© 2026 The Authors. Published by Elsevier B.V. This is an open access article under the CC BY license (<http://creativecommons.org/licenses/by/4.0/>).

compared to its affinity for iron (III) [13,14]. The high chloride activity and the presence of iron (III), which forms stable anionic species (FeCl_4^-), drive C923 to exhibit a strong preference for iron over yttrium and other REE. This behavior allows for the selective management of the high iron load while leaving others in the raffinate [15,16]. Similar to Fe, Th has also strong and stable complexes in chloride media resulting in its facile co-extraction along with Fe [17,18].

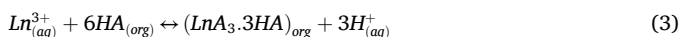
The chemical mechanism for the extraction of species from such chloride-based media by C923 typically follows a solvation pathway. For thorium the extraction is proposed as shown in Eq. (1) [19]:



Similarly, the extraction of iron proceeds via the formation of the tetrachloroferrate complex, consuming protons from leaching medium as described in Eq. (2) [20]:



Di-(2-ethylhexyl) phosphoric acid (D2EHPA) is an organophosphorus-based acidic extractant commonly used for REE separation [21–23]. It operates via a cation-exchange mechanism and is especially effective for separating HREE and LREE due to its higher separation factors for HREE in acidic solutions [24,25]. The REE extraction reaction by D2EHPA can be generalized by following Eq. (3)



The Kızılcaören deposit, which serves as the raw material source for this study, is a prominent complex ore body containing bastnasite, barite, and fluorite [26]. Several researchers have investigated the extraction potential of REE from this specific deposit using various leaching strategies, including leaching with hydrochloric acid (HCl) [27, 28], producing double sulfate salts [29], and comparing different mineral acids [30]. However, while leaching behaviors have been extensively characterized, studies focusing on the downstream solvent extraction (SX) and purification of REE specifically from this deposit remain scarce.

In this context, this study presents a self-regulating sequential solvent extraction flowsheet for the separation of HREE and LREE directly from a non-aqueous ore leachate. The fundamental novelty of this work lies in the discovery of an *in-situ* chemical conditioning mechanism within a non-aqueous matrix. While traditional aqueous-based systems require the addition of external neutralizing bases to enable LREE extraction by D2EHPA, this study exploits the synergistic dual-role of C923 in non-aqueous solvents. By selectively scavenging the massive iron impurity as an HFeCl_4 complex, C923 internally consumes protons, thereby self-regulating the leachate's acidity. To the best of our knowledge, this is the first demonstration of utilizing a solvating extractant to strategically lower the activation barrier and "unlock" the cation-exchange capacity of D2EHPA in a complex organic leachate without any external pH adjustment, paving the way for a highly selective and streamlined valorization of REE.

2. Experimental

The overall experimental flowsheet, from the initial ore treatment to the final SX experiments, is illustrated in Fig. 1. The PLS used for the SX experiments was prepared from bastnasite ore through a sequential calcination and non-aqueous leaching procedure. Initially, the raw bastnasite ore was ground to a particle size of below 25 μm and subjected to calcination at 500 °C for 8 h [31]. Subsequently, the calcined ore was leached using a non-aqueous solvent system consisting of 0.125 M FeCl_3 dissolved in EG at 75 °C for 8 h under a constant stirring speed of 300 rpm [32].

Following the leaching process, SX experiments were conducted in 3 mL glass vials (as illustrated in Fig. 2) and agitated using a horizontal shaker machine to ensure adequate mass transfer. Following the

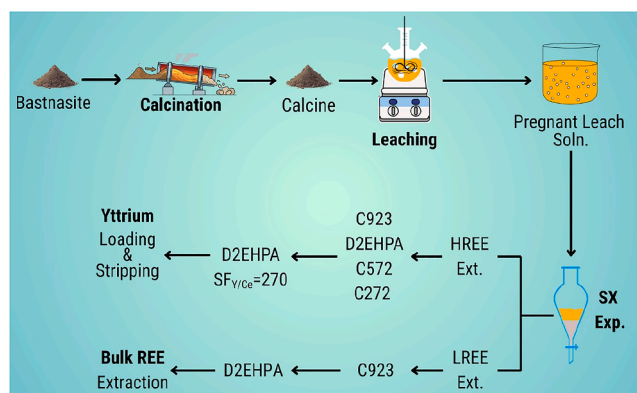


Fig. 1. Experimental flow chart.

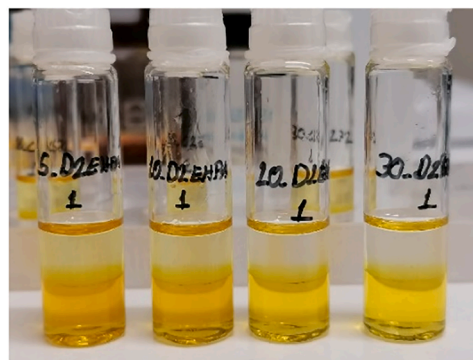


Fig. 2. Glass vials used for SX experiments.

specified shaking time, the samples were centrifuged for 5 min at 5000 rpm to ensure complete physical phase disengagement between the organic and non-aqueous EG phases. In traditional solvent extraction, the phase volume ratio is typically referred to as the organic-to-aqueous (O/A) ratio. However, since the loading stage of this study involves two organic-based phases rather than an aqueous phase, the volume ratio is denoted as the extractant-to-leachate (E/L) ratio throughout this work. Each extraction experiment was performed in triplicate to guarantee analytical reproducibility. All standard deviation values derived from these repeated experiments are presented as error bars in the respective figures; in cases where error bars are not visually apparent, the standard deviation was too small (S.D. < 0.005) to be significant.

As depicted in the overall flowsheet (Fig. 1), the SX experiments were strategically divided into two distinct operational pathways to evaluate both selective and bulk recovery strategies. The first pathway aimed to selectively extract HREE, specifically yttrium (Y), directly from the initial leachate, leaving LREE in the raffinate. An initial screening of various acidic, neutral, and solvating extractants—namely Cyanex 923 (C923), D2EHPA, Cyanex 572 (C572), and Cyanex 272 (C272)—was conducted. Based on the screening results, D2EHPA demonstrated exceptional selectivity and it was selected for the systematic optimization of Y loading and subsequent stripping parameters. The second pathway was developed to enable the extraction of LREE, an outcome that was not feasible using D2EHPA directly on the raw PLS. C923 was employed to remove iron impurities and reduce proton activity so that LREE extraction became possible. Following both *in-situ* conditioning and clearance of iron from the solvent, D2EHPA was employed to extract LREE.

3. Materials and methods

The bastnasite ore used in this study was kindly supplied by Turkish

Energy, Nuclear and Mineral Research Agency–Rare Earth Elements Research Institute (TENMAK-NATEN). Reagents like ethylene glycol (EG) and $\text{FeCl}_3 \cdot 6\text{H}_2\text{O}$ of analytical grade were used. The extractants C923, C572, and C272 were supplied by Solvay, and bis(2-ethylhexyl) phosphate (D2EHPA) was supplied by Merck. Solvent 70 (Statoil), an aliphatic kerosene derivative distilled at 190–250 °C, was used as a diluent.

Elemental concentrations in the respective phases were determined using Inductively Coupled Plasma Optical Emission Spectrometry (ICP-OES, Thermo iCAP 6500). The extraction percentage (%E), distribution ratio (D_M), and separation factor (SF) were calculated according to Equations 4, 5, and 6, respectively.

$$\text{Extraction Percentage (\%)} = \frac{[M]_{\text{Stock}} - [M]_{\text{Raffinate}}}{[M]_{\text{Stock}}} \times 100 \quad (4)$$

$$\text{Distribution Ratio of Metal M } (D_M) = \frac{[M]_{\text{org}}}{[M]_{\text{EG}}} \quad (5)$$

$$\text{Separation Factor of Metal M over Metal N } (SF_{MN}) = \frac{D_M}{D_N} \quad (6)$$

In these equations, $[M]_{\text{Stock}}$ and $[M]_{\text{Raffinate}}$ represent the initial metal concentration in the feed solution and the final metal concentration in the EG raffinate phase, respectively. Similarly, $[M]_{\text{org}}$ and $[M]_{\text{EG}}$ denote the equilibrium concentrations of the target metal in the loaded organic phase and the EG phase, while D_M and D_N refer to the distribution ratios of the specific metals being separated.

To validate the presence and changes of chemical bonds, the samples were analyzed by FTIR spectroscopy using PerkinElmer Spectrum Two equipment with a resolution of 4 cm^{-1} at room temperature. Transmission spectra were traced between 400 and 4000 cm^{-1} . For both pure compounds and mixtures, bindings, especially hydrogen, and $P = O$ bonds were identified by observing shifts, formation, and disappearance of characteristic transmittance bands. These shifts indicate interactions between molecules in the mixtures, providing evidence for loading of metal ions onto the extractants.

4. Results and discussion

4.1. Separation of HREE and LREE (Pathway1)

Throughout experimental studies, PLS obtained as explained in experimental section was used as a REE stock, and its metal concentration is given Table 1. First pathway, as described in Fig. 1, aims to find a highly selective extractant for the separation of HREE, LREE. Four different solvents (C923, C572, C272, D2EHPA) diluted in Solvent-70 were shaken for 30 min at a fixed volume ratio to 1/1. Following completing experiments, samples were centrifuged, and metal concentrations in leachate were analyzed to calculate extraction percentages of REE given in Fig. 3.

In this study, yttrium (Y) and cerium (Ce) were selected as the primary representative elements for HREE and LREE, respectively. As illustrated in Fig. 3, while all evaluated extractants exhibited high extraction efficiencies for Fe and Th, only D2EHPA successfully extracted Y. Furthermore, Fig. 4 demonstrates that the separation factor of Y over Ce ($SF_{Y/Ce}$) reached a maximum of 270.4 when 30 vol.% D2EHPA was utilized. This distinct behavior highlights D2EHPA as a highly suitable and selective extractant for this non-aqueous system. Additionally, the co-extraction of other impurity ions (e.g., Ca, Ba) was negligible across all tested extractants, which is an advantage for

producing a high-purity REE solution during the subsequent stripping stage.

The optimization of yttrium extraction parameters, specifically contact time, shaking speed, and E/L volume ratio is presented in Fig. 5. As shown in Fig. 5A, although the highest mean Y extraction (93 %) was observed at 10 min, the large error bars indicate low reproducibility. Extending the contact time to 30 min resulted in a slight decrease in yield (to 90 %) but provided significantly more robust and reproducible data. Since increasing the time further to 60 min yielded no additional benefit, 30 min was selected as the optimal duration. Subsequent trials on shaking speed (Fig. 5B) and E/L ratio (Fig. 5C) demonstrated that higher shaking speeds (2000 rpm) and a 2:1 vol.ratio maximized recovery, reaching 97 % extraction. Consequently, the optimal conditions were determined as 30 min shaking time, 2000 rpm shaking speed, and a 2:1 E/L ratio.

Slope Analysis: The slope analysis method ($\log[D]$ vs. $\log[\text{Extractant}]$) is a powerful tool widely used in the literature for determining stoichiometric coefficients. However, this method is valid for ideal, single-metal systems. In multi-component systems such as in our study (containing Fe^{3+} , Th^{4+} , and Y^{3+}), there is strong competition for the extractant (D2EHPA). As given in Fig. 6, the slope for Y, Th, and Fe is approximately 2, 1, 1, respectively. This result is in contradiction of literature-based knowledge. However, the presence of metals such as Fe^{3+} and Th^{4+} , which are extracted at much lower pH values than Y^{3+} , dramatically affects the free concentration of D2EHPA (extractant loading) and invalidates the fundamental assumptions of the method. Due to this competitive loading, the obtained slope for yttrium (slope=2) does not reflect the true stoichiometric ratio but rather represents an 'apparent' value. Therefore, rather than a stoichiometric analysis of our system, the focus has been placed on the practical effects of pH and extractant concentration on separation efficiency.

Stripping studies: Following the optimization of HREE extraction, a bulk extraction experiment was conducted to prepare a sufficient volume of loaded organic phase for subsequent stripping studies. The leachate was contacted with 30 vol.% D2EHPA at an O/A ratio of 1:1 by hand-shaking for 10 min. As seen in Fig. 7, although the high viscosity of the EG medium resulted in a relatively slower phase disengagement initially compared to typical aqueous systems, a clear and complete phase separation was successfully achieved within 10 min, demonstrating the physical feasibility of the process without any crud formation. The EG based raffinate was analyzed (Table 2) to confirm the successful loading of HREE (Y) into the organic phase, while leaving most LREE (La, Ce, Nd) in EG phase.

Initial stripping experiments were performed to identify the most suitable stripping agent for the recovery of yttrium from the loaded D2EHPA. Three mineral acids (HCl, HNO_3 , H_2SO_4) and deionized water were tested. The experiments were conducted at a fixed O/A ratio of 1:1, with a shaking time of 30 min at 1000 rpm. The results, presented in Table 3, clearly indicate that nitric acid is the most efficient stripping agent for yttrium among tested agents.

Using 2 M HNO_3 yielded a Y stripping efficiency of 59.84 %, with negligible stripping of Th (<0.05 %). HCl and H_2SO_4 showed significantly lower Y stripping efficiencies (10.70 % and 9.44 %, respectively). Deionized water resulted in no measurable stripping. Consequently, HNO_3 was selected for further optimization (Table 3).

Further optimization of Y stripping with HNO_3 was conducted by investigating the effects of acid concentration (0.5 – 3.0 M) and organic-to-aqueous (O/A) volume ratio. The results (Fig. 8) demonstrate that increasing both the HNO_3 concentration and the volume of the aqueous stripping phase (i.e., decreasing O/A ratio) significantly enhances Y

Table 1
Stock solution concentration in ppm.

Ce	La	Nd	Pr	Th	Y	Ca	Ba	Fe
654.55	599.12	85.36	55.88	10.10	1.70	177.18	41.60	7498.5

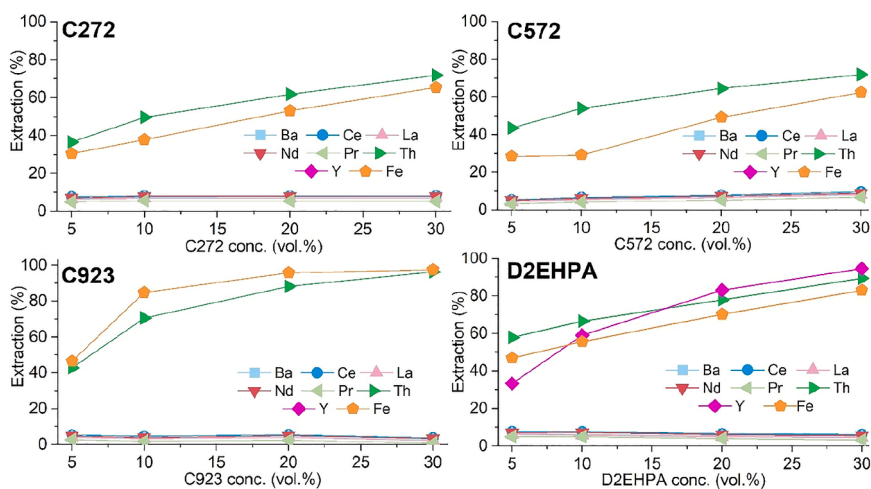


Fig. 3. Solvent type comparison for separation of HREE, and LREE (Contact time: 30 min., E/L:1/1).

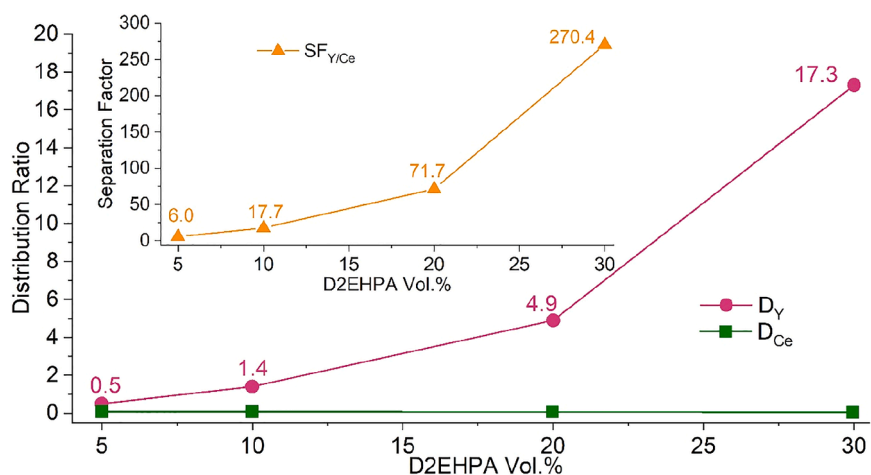


Fig. 4. Distribution ratio, and separation factor of Y, Ce (Contact time: 30 min., E/L:1/1).

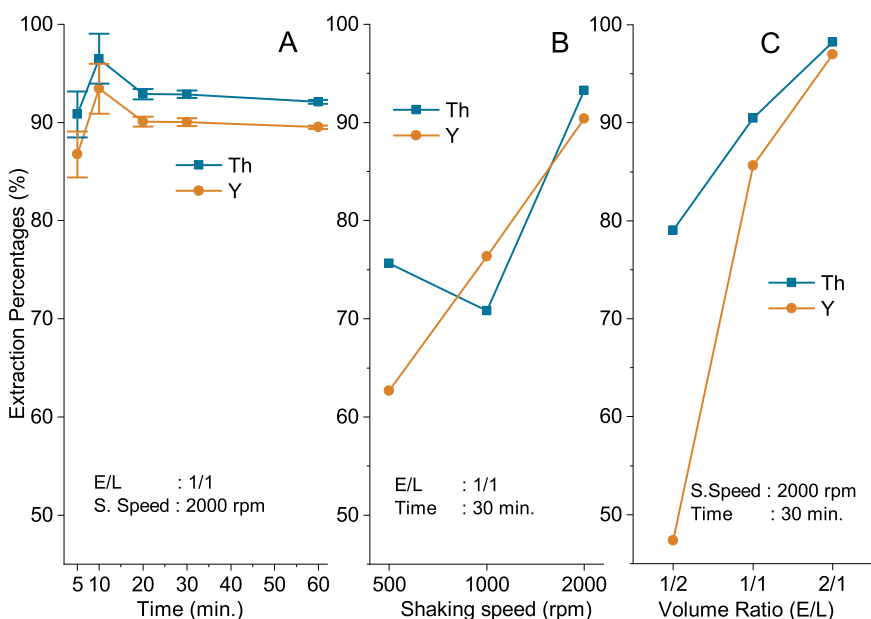


Fig. 5. Yttrium extraction optimization graphs A) shaking time B) shaking speed C) volume ratio.

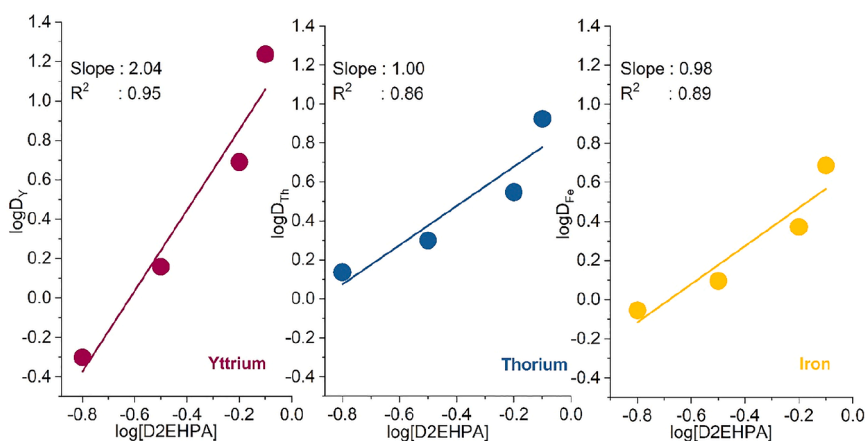


Fig. 6. Plot for $\log [D_{Y, Th, Fe}]$ vs. $\log [D2EHPA]$.

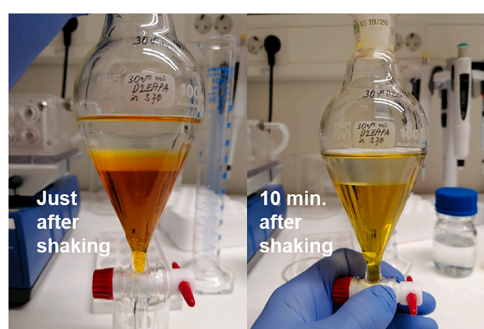


Fig. 7. Phase separation during bulk extraction for loaded organic preparation.

Table 2

Chemical composition of the raffinate after HREE extraction (ppm).

Ba	Ca	Ce	La	Nd	Pr	Th	Y
40.05	159.54	633.40	579.65	82.73	54.79	0.94	0.23

Table 3

Preliminary stripping experiments' results in wt.%.

Stripping Agent	Ce	La	Nd	Th	Y
2M-HNO ₃	0.72	0.18	2.99	0.05	59.84
2M-HCl	0.74	0.13	5.63	1.16	10.70
2M- H ₂ SO ₄	0.47	0.03	6.05	11.17	9.44
Water	No Stripping				

stripping efficiency.

The highest Y stripping efficiency of 87.44 % was achieved using 3 M HNO₃ at an O/A ratio of 1:2 in one step. The chemical composition of the final product solution obtained under these optimal conditions is given in Table 4.

As seen in Table 4, a highly selective separation of Y from other REE and Th was achieved. Concentrations of Ce, La, Nd, Pr, and Th were mostly below detection limits. Although some iron co-stripping occurred (3.83 ppm), producing a final solution with Fe impurity, the primary goal of separating yttrium from other REE and thorium was successfully met. A subsequent purification step (e.g., precipitation) could be applied to remove residual iron if higher purity is required.

4.2. Synergistic effect of C923 (Pathway 2)

To address the significant iron impurity in the final product, the

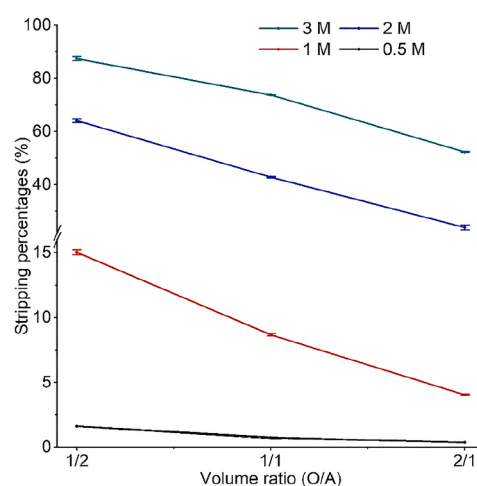


Fig. 8. Effect of HNO₃ concentration and O/A ratio on Y stripping efficiency.

Table 4

Chemical composition of the optimized stripping solution in ppm (3 M HNO₃, O/A = 1:2).

Ba	Ca	Ce	La	Nd	Pr	Th	Y	Fe
0.001	< LOD	< LOD	< LOD	0.044	< LOD	< LOD	0.651	3.831

flowsheet was revised to include a pre-extraction stage using the neutral solvating extractant C923 prior to the main D2EHPA extraction. The primary objective was to selectively remove Fe as the HFeCl₄ complex, providing an iron-free leachate to yield a high-purity yttrium product. While C923 successfully removed >95 % of the iron, it also triggered an unexpected mechanistic shift in the subsequent D2EHPA stage. In the original highly acidic leachate, the excessive proton activity severely suppressed the cation-exchange mechanism of D2EHPA, rendering it incapable of extracting LREE. However, because C923 extracts iron specifically in the form of the acidic HFeCl₄ complex, it effectively acts as a proton sink, thereby reducing the overall acidity of the non-aqueous matrix. When D2EHPA was applied to this acid-conditioned raffinate, it not only maintained high extraction efficiency for Y but also successfully co-extracted the LREE (79 % La, 89 % Ce, and 92 % Nd). This reveals a synergistic mechanism where C923 dual-functions as both an iron purification and an in-situ acid-conditioning agent, ultimately unlocking the comprehensive recovery of all REE.

The fundamental reason why D2EHPA failed to extract LREE from

the initial leachate, yet successfully co-extracted them after the C923 stage, can be directly attributed to a significant reduction in matrix acidity. In conventional aqueous systems, such a macroscopic pH shift following C923 extraction would not be possible. This is because the vast excess of bulk water acts as a massive thermodynamic buffer, effectively neutralizing and masking any proton depletion. However, in the proposed non-aqueous system, the selective removal of the acidic HFeCl_4 complex by C923 directly consumes protons. Without an aqueous buffer layer, this mechanism effectively lowers the system's acidity to an optimal range for LREE extraction by the acid-sensitive D2EHPA. While confirming this phenomenon through direct potentiometric pH measurements would be ideal, pH determination in non-aqueous and DES-like media is notoriously challenging and currently lacks a standardized methodology [33]. Consequently, the mechanism behind this in-situ acidity reduction is further elucidated through bond vibrations by FTIR spectroscopic analysis in the following section.

4.3. Extraction mechanism analysis through bond vibrations

FTIR spectroscopic analysis provided critical evidence for the chemical mechanisms at play during the multi-stage extraction process. This analysis examined changes in both the organic extractant phases

(Fig. 9) and EG leachate phase (Fig. 10).

The analysis of the organic phases confirmed distinct metal-binding mechanisms for each extractant. The spectrum of 30 vol. % D2EHPA in solvent 70 clearly shows D2EHPA characteristic peaks as the broad, shallow acidic P-O-H bands ($\sim 1600\text{--}2400\text{ cm}^{-1}$), P-O band at 1030 cm^{-1} , and the strong phosphoryl (P = O) peak at 1228 cm^{-1} . In the spectrum of D2EHPA after extraction, broad P-O-H bands completely disappear, confirming the release of the acidic proton (H^+). Simultaneously, the P = O peak shifts significantly from 1228 cm^{-1} to 1200 cm^{-1} , a classic indicator of the phosphoryl oxygen coordinating to a metal cation. Additionally, the strong P-O-C band at $\sim 1030\text{ cm}^{-1}$ remains in the same position but shows a clear increase in absorbance (decrease in transmittance) after extraction, further indicating the formation of a new metal-organic complex that alters the dipole moment of the phosphate ester backbone.

In contrast, the mechanism for C923 was different. As it is a commercial mixture, it is difficult to identify its characteristic peaks as precisely as those of D2EHPA. However, key changes are still clearly discernible. The spectrum of 30 vol. % C923 in solvent 70 shows characteristic C-H bending vibrations from the alkyl chains at $\sim 1460\text{ cm}^{-1}$ (CH_2) and $\sim 1378\text{ cm}^{-1}$ (CH_3), which remain stable after extraction. A small characteristic free P = O band is discernible at $\sim 1156\text{ cm}^{-1}$. Upon

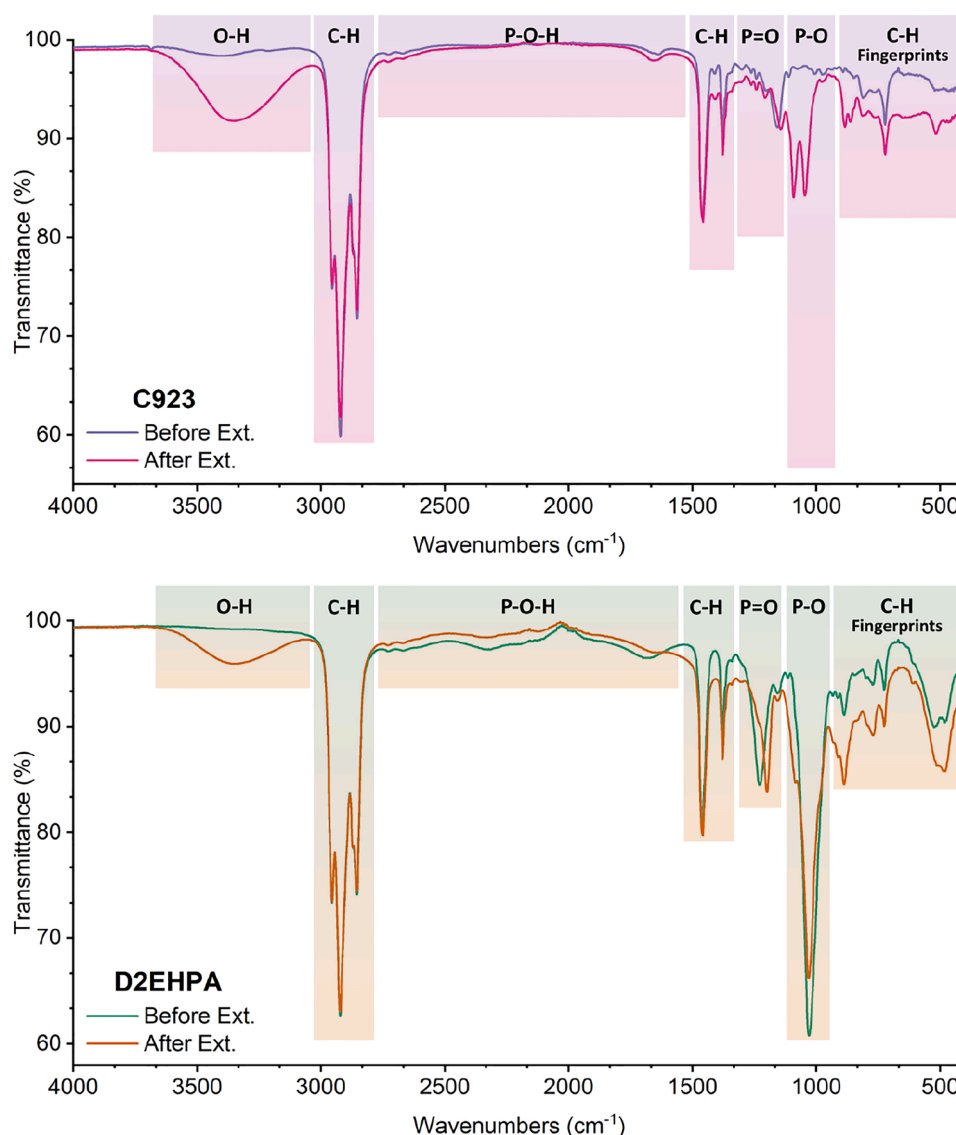


Fig. 9. FTIR spectra of D2EHPA, and C923 before and after extraction.

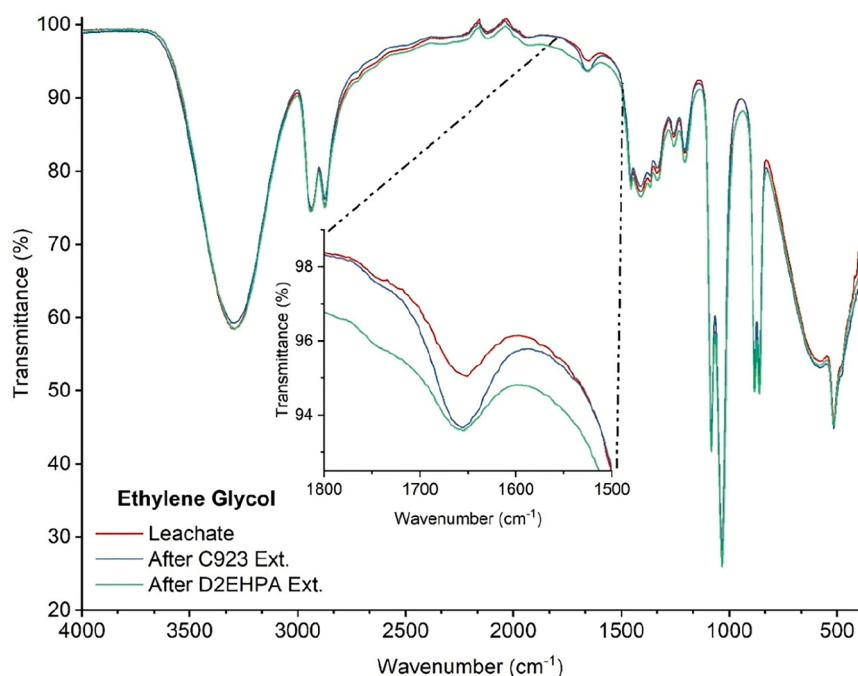


Fig. 10. FTIR spectra of ethylene glycol before, and after extraction.

extraction, this band shifts to $\sim 1144\text{ cm}^{-1}$, indicating metal coordination. Concurrently, the formation of entirely new peaks at around 1045 cm^{-1} and 1092 cm^{-1} represents the strong coordination of the phosphoryl oxygen with the extracted chloro-complex (HFeCl_4) as suggested by different authors [34,35].

Furthermore, both the D2EHPA and C923 spectra after extraction show a new, broad transmittance band appearing between $3000\text{--}4000\text{ cm}^{-1}$, corresponding to O—H stretching vibrations. This indicates the co-extraction (or entrainment) of trace amounts of water and/or EG from the leachate into the organic phase. It is critical to note that no macroscopic, visually observable solvent loss was detected (i.e., the phase boundary line did not change). The significant intensity of this O—H band, despite the immeasurably small volume, is attributed to the very high molar absorptivity (signal strength) of the polar O—H bond, which can produce a strong signal even at trace levels.

Analysis of EG leachate phase itself confirmed the stability of the solvent and the consequences of each extraction. The spectrum (Fig. 10) of the initial leachate, and after both extractions show the main EG peaks (e.g., C—O stretches at $\sim 1040\text{--}1080\text{ cm}^{-1}$) in the same position, confirming the chemical stability of the solvent throughout the process. However, the byproducts of each reaction were evident. The spectrum of the leachate after D2EHPA extraction exhibits a clear decrease in transmittance (increased absorbance) across the entire broad region from $1500\text{--}2500\text{ cm}^{-1}$ when compared to the initial leachate. This is the characteristic "acid band" caused by the solvated protons (H^+) released by D2EHPA during ion exchange, chemically suggesting that the extraction occurred. Conversely, the spectrum of the leachate after C923 extraction exhibits a sharper and deeper peak (higher net absorbance) at the H_2O bending vibration ($\sim 1650\text{ cm}^{-1}$) compared to both the initial leachate and the D2EHPA raffinate. This indicates a higher concentration of "free" water molecules in the C923 raffinate, a result of the differing secondary effects of the two extractants on solution acidity. While both extractants initially release water molecules by stripping them from the hydration spheres of extracted Fe^{3+} ions, their subsequent interaction with these water molecules diverges. D2EHPA, being an acidic extractant, releases protons (H^+) that immediately react with and consume these newly released free water molecules to form hydronium (H_3O^+) ions, thereby suppressing the water signal. Basically,

D2EHPA consumes the water molecules produced from iron extraction through its acidic mechanism, whereas the neutral character of C923 allows these water molecules to remain free, resulting in a visibly higher water concentration signal in its EG raffinate. While spectroscopic data supports our findings, the lack of direct acidity measurements in this non-aqueous system remains a limitation to be addressed in future proton activity/speciation studies.

4.4. Initial Scale-up challenges and advantages

A primary engineering challenge in non-aqueous solvent extraction is the high viscosity of the medium, which typically hinders mass transfer and phase disengagement. While conventional aqueous systems utilizing D2EHPA often achieve complete phase separation within few minutes, the settling kinetics in the EG matrix are inherently slower. However, the use of hydrated iron chloride ($\text{FeCl}_3 \cdot 6\text{H}_2\text{O}$) and release of hydration water during leaching, and SX effectively reduced the viscosity of the leachate to approximately 9 cP from 16 cP. Consequently, a clear phase separation was practically achieved within maximum 10 min without any observable crud formation (Fig. 7). This settling time is an initial estimate and measured in a separating funnel (vertical shape) and consequently can be improved by a proper settling pool geometry (horizontal shape) and further optimizing the volume ratio of solvents. Furthermore, considering that continuous mixer-settler operations have been successfully demonstrated in recent literature for non-aqueous systems with viscosities as high as 156 cP [7], the 9 cP viscosity of conditioned EG matrix proves to be highly manageable and exceptionally favorable for practical scale-up. Beyond physical feasibility, C923 in-situ pH regulation entirely eliminates the need for external neutralizing agents which generally causes crud formation in mixer settler systems. It must be emphasized that these observations regarding rapid phase separation, viscosity reduction, and the lack of crud formation serve strictly as preliminary proof-of-concept indicators. Validated long-term process performance and solvent recyclability require future continuous mixer-settler operations.

5. Conclusion

In this study, REE were successfully leached from bastnaesite ore calcine using an EG-based solvent system. D2EHPA was identified as a highly effective extractant for this system, capable of selectively separating HREE (Y) from LREE (Ce) with a high separation factor of 270 from the original leachate. Stripping of the loaded D2EHPA with 3 M HNO₃ achieved 87.4 % Y recovery, demonstrating excellent separation from other REE and Th, but revealed significant Fe contamination. FTIR spectroscopy provided strong molecular-level indicators for the extraction mechanisms. D2EHPA's ion-exchange was confirmed by the disappearance of P-O-H bands and a shift in the P = O peak (from 1228 cm⁻¹ to 1200 cm⁻¹). C923's complexation was shown by the emergence of new, strong absorbance peaks (~1045 cm⁻¹, ~1092 cm⁻¹) strongly suggesting the formation of chloro-complexes. Furthermore, FTIR analysis of the raffinates confirmed that D2EHPA releases H⁺ (acidifies), while C923's mechanism results in a higher concentration of "free" H₂O, indicating a reduction in leachate acidity. This investigation led to a critical discovery: a two-stage process, initially designed to remove Fe using C923, also acted as a vital process conditioning step. The C923 pre-extraction was found to co-extract acid (HFeCl₄), raising the leachate pH. This conditioning unlocked the ability of D2EHPA to perform LREE extraction, a feat not possible from the original medium.

In conclusion, this work presents two distinct pathways for EG-based systems: a selective HREE route using D2EHPA alone, and a novel synergistic process for bulk REE recovery, enabled by the dual-function (purification and pH conditioning) of C923. Beyond the specific mineralogy of the studied deposit, these findings hold global relevance for the sustainable processing of complex REE resources. The process conditioning capability of C923 in non-aqueous systems offers a promising approach for managing acidity and high-iron matrices without external base addition which generally causes crud formation problems. Consequently, this synergistic flowsheet could serve as a potential blueprint for diverse REE sources worldwide, warranting further investigation into its applicability to other primary or secondary sources.

Declaration of generative AI and AI-assisted technologies

During the preparation of this work the authors used Gemini in order to increase the readability of the paper. After using this tool, the authors reviewed and edited the content as needed and take full responsibility for the content of the published article.

Funding information

This study has two fundings one is from Turkish Energy, Nuclear and Mineral Research Agency– Rare Earth Elements Research Institute (TENMAK-NATEN) (Project No: A2.H1.P20), and other one is from Istanbul Technical University BAP division (Project No: MDK-2022–43727). Also, Ş. Samet Kaplan has received a fellowship from TUBITAK under 2214-A - International Research Fellowship Programme for PhD Students.

CRediT authorship contribution statement

S.Samet Kaplan: Writing – original draft, Visualization, Methodology, Investigation. **M.Seref Sonmez:** Writing – review & editing, Supervision, Funding acquisition. **Martina Petranikova:** Writing – review & editing, Supervision, Funding acquisition.

Declaration of competing interest

The authors declare that they have no known competing financial interests or personal relationships that could have appeared to influence the work reported in this paper.

Acknowledgments

Authors would like to acknowledge that this study is financially supported by Turkish Energy, Nuclear and Mineral Research Agency– Rare Earth Elements Research Institute (TENMAK-NATEN) (Project No: A2.H1.P20), and Istanbul Technical University BAP division (Project No: MDK-2022–43727). For FTIR analysis, authors would like to thank Prof. Dr. Bihter Zeytuncu Gökoğlu, and her team. Also, TUBITAK is acknowledged for the support under 2214-A - International Research Fellowship Programme for PhD Students.

Data availability

Data will be made available on request.

References

- [1] F. Sadri, A.M. Nazari, A. Ghahreman, A review on the cracking, baking and leaching processes of rare earth element concentrates, *J. Rare Earths* 35 (2017) 739–752, [https://doi.org/10.1016/S1002-0721\(17\)60971-2](https://doi.org/10.1016/S1002-0721(17)60971-2).
- [2] P. Cen, X. Bian, Z. Liu, M. Gu, W. Wu, B. Li, Extraction of rare earths from bastnaesite concentrates: a critical review and perspective for the future, *Min. Eng.* 171 (2021) 107081, <https://doi.org/10.1016/J.MINENG.2021.107081>.
- [3] J. Kim, J. Choi, S. Lee, A review of rare Earth elements recovery from Bastnaesite ore: from beneficiation to metallurgical processing, *J. Sustain. Metall.* 2025 11 2 (11) (2025) 773–798, <https://doi.org/10.1007/S40831-025-01019-0>.
- [4] K. Binnemans, P.T. Jones, Solvometallurgy: an emerging branch of extractive metallurgy, *J. Sustain. Metall.* 3 (2017) 570–600, <https://doi.org/10.1007/s40831-017-0128-2>.
- [5] E.L. Smith, A.P. Abbott, K.S. Ryder, Deep eutectic solvents (DESs) and their applications, *Chem. Rev.* 114 (2014) 11060–11082, <https://doi.org/10.1021/cr300162p>.
- [6] E. Güloğlu, G. Orhan, Solvleaching and kinetic approach of end-of-life lithium-ion battery cathode active powder in DL-malic–Based DESs, *mining, Metall. Explor.* 6 (42) (2025) 4045–4059, <https://doi.org/10.1007/S42461-025-01386-Y>.
- [7] S. Riaño, M. Petranikova, B. Onghena, T. Vander Hoogerstraete, D. Banerjee, M.R. St.J. Foreman, C. Ekberg, K. Binnemans, Separation of rare earths and other valuable metals from deep-eutectic solvents: a new alternative for the recycling of used NdFeB magnets, *RSC. Adv.* 7 (2017) 32100–32113, <https://doi.org/10.1039/C7RA06540J>.
- [8] A.P. Abbott, J.C. Barron, K.S. Ryder, D. Wilson, Eutectic-based ionic liquids with metal-containing anions and cations, *Chem. - Eur. J.* 13 (2007) 6495–6501, <https://doi.org/10.1002/chem.200601738>.
- [9] X. Li, W. Monnens, Z. Li, J. Franssaer, K. Binnemans, Solvometallurgical process for extraction of copper from chalcocite and other sulfidic ore minerals, *Green Chem.* 22 (2020) 417–426, <https://doi.org/10.1039/C9GC02983D>.
- [10] E. Dziwiński, J. Szymanowski, Composition of CYANEX® 923, CYANEX® 925, CYANEX® 921 and TOPO, *Solvent Extr. Ion Exch.* 16 (1998) 1515–1525, <https://doi.org/10.1080/07366299808934592>.
- [11] S. Spathariotis, N. Peeters, K.S. Ryder, A.P. Abbott, K. Binnemans, S. Riaño, Separation of iron(III), zinc(II) and lead(II) from a choline chloride–ethylene glycol deep eutectic solvent by solvent extraction, *RSC. Adv.* 10 (2020) 33161–33170, <https://doi.org/10.1039/D0RA06091G>.
- [12] B. Gupta, P. Malik, A. Deep, Solvent extraction and separation of trivalent lanthanides and yttrium using Cyanex 923, *Solvent Extr. Ion Exch.* 21 (2003) 239–258, <https://doi.org/10.1081/SEI-120018948>.
- [13] N.K. Batchu, T. Vander Hoogerstraete, D. Banerjee, K. Binnemans, Separation of rare-earth ions from ethylene glycol (+LiCl) solutions by non-aqueous solvent extraction with Cyanex 923, *RSC. Adv.* 7 (2017) 45351–45362, <https://doi.org/10.1039/C7RA09144C>.
- [14] B. Dewulf, N.K. Batchu, K. Binnemans, Enhanced separation of neodymium and dysprosium by nonaqueous solvent extraction from a polyethylene glycol 200 phase using the neutral extractant cyanex 923, *ACS Sustain. Chem. Eng.* 8 (2020) 19032–19039, <https://doi.org/10.1021/acsschemeng.0c07207>.
- [15] K. Larsson, C. Ekberg, A. Ødegaard-Jensen, Using Cyanex 923 for selective extraction in a high concentration chloride medium on nickel metal hydride battery waste: part II: mixer–settler experiments, *Hydrometallurgy* 133 (2013) 168–175, <https://doi.org/10.1016/J.HYDROMET.2013.01.012>.
- [16] D. Lloyd, T. Vainikka, M. Ronkainen, K. Kontturi, Characterisation and application of the Fe(II)/Fe(III) redox reaction in an ionic liquid analogue, *Electrochim. Acta* 109 (2013) 843–851, <https://doi.org/10.1016/J.ELECTACTA.2013.08.013>.
- [17] E.L. Zebroski, H.W. Alter, F.K. Heumann, R.W. Young, B.E.L. Zebroski, Thorium Complexes with Chloride, Fluoride, Nitrate, Phosphate and Sulfate, 1948.
- [18] J.N. Wacker, M. Vasiliu, I. Colliard, R.L. Ayscue, S.Y. Han, J.A. Bertke, M. Nyman, D.A. Dixon, K.E. Knope, Monomeric and trimeric thorium chlorides isolated from acidic aqueous solution, *Inorg. Chem.* 58 (2019) 10871–10882, <https://doi.org/10.1021/ACS.INORGCHEM.9B01238>.
- [19] H. Wang, S. Kuang, W. Liao, Synergistic extraction and separation of thorium from rare earths in chloride media using mixture of Cextrant 230 and Cyanex 923, *J. Rare Earths* 42 (2024) 759–767, <https://doi.org/10.1016/J.JRE.2023.04.016>.

- [20] S. Spathariotis, N. Peeters, K.S. Ryder, A.P. Abbott, K. Binnemans, S. Riä, Separation of iron(III), zinc(II) and lead(II) from a choline chloride-ethylene glycol deep eutectic solvent by solvent extraction, (2020). <https://doi.org/10.1039/d0ra06091g>.
- [21] M. Mohammadi, K. Forsberg, L. Kloof, J. Martinez De La Cruz, Å. Rasmuson, Separation of Nd(III), Dy(III) and Y(III) by solvent extraction using D2EHPA and EHEHPA, *Hydrometallurgy* 156 (2015) 215–224, <https://doi.org/10.1016/j.hydromet.2015.05.004>.
- [22] S. Pavón, A. Fortuny, M.T. Coll, A.M. Sastre, Solvent extraction modeling of Ce/Eu/Y from chloride media using D2EHPA, *AIChE J.* 65 (2019) e16627, <https://doi.org/10.1002/AIC.16627;PAGE=STRING:ARTICLE/CHAPTER>.
- [23] S.G. Song, J.H. Jeon, M.S. Lee, Comparison of solvent extraction of Nd(III) from hydrochloric acid solution containing Ce(III) and La(III) between D2EHPA and its ionic liquid synthesized with Aliquat 336, *Miner. Process. Extr. Metall. Rev.* 46 (2025) 957–967, <https://doi.org/10.1080/08827508.2025.2547193>.
- [24] M. Gergoric, C. Ekberg, B.M. Steenari, T. Retegan, Separation of heavy rare-earth elements from light rare-earth elements via solvent extraction from a neodymium magnet leachate and the effects of diluents, *J. Sustain. Metall.* 3 (2017) 601–610, <https://doi.org/10.1007/S40831-017-0117-5/FIGURES/4>.
- [25] B. Dewulf, S. Riaño, K. Binnemans, Separation of heavy rare-earth elements by non-aqueous solvent extraction: flowsheet development and mixer-settler tests, *Sep. Purif. Technol.* 290 (2022) 120882, <https://doi.org/10.1016/j.seppur.2022.120882>.
- [26] A.H. Gültekin, Y. Örgün, F. Suner, Geology, mineralogy and fluid inclusion data of the Kizilcaören fluorite–barite–REE deposit, Eskisehir, Turkey, *J. Asian Earth Sci.* 21 (2003) 365–376, [https://doi.org/10.1016/S1367-9120\(02\)00019-6](https://doi.org/10.1016/S1367-9120(02)00019-6).
- [27] I. Kursun, M. Terzi, T.D. Tombal, HCl leaching behaviour of a bastnasite ore in terms of thorium and rare Earth elements 1, *Russ. J. Non-Ferr. Met.* 57 (2016) 187–194, <https://doi.org/10.3103/S106782121603010X>.
- [28] H. Güneş, H.E. Obuz, H. Akçay, Ç. Kara, A. Erdem, Production of rare-earth oxides from Eskişehir-Beylikova complex ores, *Bull. Miner. Res. Explor.* 170 (2023) 87, <https://doi.org/10.19111/bulletinofmre.1180222>.
- [29] M. Kul, Y. Topkaya, I. Karakaya, Rare earth double sulfates from pre-concentrated bastnasite, *Hydrometallurgy* 93 (2008) 129–135, <https://doi.org/10.1016/J.HYDROMET.2007.11.008>.
- [30] S. Kursunoglu, S. Top, S. Hussaini, H.S. Gokcen, M. Altiner, S. Ozsarac, M. Kaya, Extraction of lanthanum and cerium from a Bastnasite ore by direct acidic leaching, *Bilimsel Madencilik Derg.* 59 (2020) 85–92, <https://doi.org/10.30797/MADENCILIK.757979>.
- [31] S.S. Kaplan, C.C. Kurtulan, S. Gurmen, G. Orhan, M.S. Sonmez, Influence of calcination conditions on deep eutectic solvents (DES) leaching efficiency of light rare earth elements in bastnasite ore, *Min. Eng.* 220 (2025), <https://doi.org/10.1016/j.mineng.2024.109087>.
- [32] S.S. Kaplan, M.S. Sonmez, M. Petranikova, Extraction of rare earth elements from Bastnasite Ore and separation of heavy REEs and light REEs by solvent Extraction, *minerals, Met. Mater. Ser.* (2025) 59–66, https://doi.org/10.1007/978-3-031-81182-1_7.
- [33] V. Jancíková, V. Majová, M. Jablonský, Acidity and pH of DES-like mixtures and the possibilities of their determination, *J. Mol. Liq.* 394 (2024) 123728, <https://doi.org/10.1016/j.molliq.2023.123728>.
- [34] J. Tu, X. Feng, B. Zhang, L. Chen, From waste to added-value product: a case of efficient separation and recovery of zinc and iron from spent galvanizing acid, *Prog. Nat. Sci.: Mater. Int.* 34 (2024) 702–709, <https://doi.org/10.1016/j.pnsc.2024.06.005>.
- [35] F.J. Alguacil, F.A. López, The extraction of mineral acids by the phosphine oxide cyanex 923, *Hydrometallurgy* 42 (1996) 245–255, [https://doi.org/10.1016/0304-386X\(95\)00101-L](https://doi.org/10.1016/0304-386X(95)00101-L).